

## Development of a ReaxFF Reactive Force Field for Aqueous Chloride and Copper Chloride

Obaidur Rahaman,<sup>†</sup> Adri C. T. van Duin,<sup>‡</sup> Vyacheslav S. Bryantsev,<sup>§</sup> Jonathan E. Mueller,<sup>§</sup> Santiago D. Solares,<sup>||</sup> William A. Goddard III,<sup>§</sup> and Douglas J. Doren<sup>\*,†</sup>

Department of Chemistry and Biochemistry, University of Delaware, Newark, Delaware 19716, Department of Mechanical and Nuclear Engineering, The Pennsylvania State University, University Park, Pennsylvania 16802, Material and Process Simulation Center, California Institute of Technology, Pasadena, California 91125, and Department of Mechanical Engineering, University of Maryland, College Park, Maryland 20742

Received: September 18, 2009; Revised Manuscript Received: January 11, 2010

Copper ions play crucial roles in many enzymatic and aqueous processes. A critical analysis of the fundamental properties of copper complexes is essential to understand their impact on a wide range of chemical interactions. However the study of copper complexes is complicated by the presence of strong polarization and charge transfer effects, multiple oxidation states, and quantum effects like Jahn–Teller distortions. These complications make the experimental observations difficult to interpret. In order to provide a computationally inexpensive yet reliable method for simulation of aqueous-phase copper chemistry, ReaxFF reactive force field parameters have been developed. The force field parameters have been trained against a large set of DFT-derived energies for condensed-phase copper–chloride clusters as well as chloride/water and copper–chloride/water clusters sampled from molecular dynamics (MD) simulations. The parameters were optimized by iteratively training them against configurations generated from ReaxFF MD simulations that are performed multiple times with improved sets of parameters. This cycle was repeated until the ReaxFF results were in accordance with the DFT-derived values. We have performed MD simulations on chloride/water and copper–chloride/water systems to validate the optimized force field. The structural properties of the chloride/water system are in accord with previous experimental and computational studies. The properties of copper–chloride/water agreed with the experimental observations including evidence of the Jahn–Teller distortion. The results of this study demonstrate the applicability of ReaxFF for the precise characterization of aqueous copper chloride. This force field provides a base for the design of a computationally inexpensive tool for the investigation of various properties and functions of metal ions in industrial, environmental, and biological environments.

### 1. Introduction

Copper complexes play important roles in industrial processes and the active sites of many enzymes involved in oxygen transport, electron transfer, and oxidation–reduction reactions.<sup>1,2</sup> A comprehensive study of the properties of copper complexes is essential to understand the intricate molecular mechanisms which are critical for their functions. The  $d^9$  ( $t_{2g}^6e_g^3$ ) electronic configuration of the  $\text{Cu}^{2+}$  ion suggests a Jahn–Teller distorted<sup>3</sup> octahedral coordination geometry with four equidistant equatorial ligands and two elongated axial ligands. Despite numerous experimental<sup>4–12</sup> and theoretical studies<sup>13–21</sup> devoted to this problem, the coordination number and geometry of the most common ion,  $\text{Cu}^{2+}$ , in aqueous solution remains ambiguous. Different experimental studies support 5-fold,<sup>11,12</sup> 6-fold,<sup>8</sup> or a coexistence of different coordination numbers<sup>10</sup> for the aqueous  $\text{Cu}^{2+}$ . There is no consensus among the computational studies as well. Car–Parrinello molecular dynamics (CPMD) simulations and neutron diffraction studies predict a 5-fold coordination with interchanging square pyramidal and trigonal bipyramidal geometries.<sup>13</sup> The 5-fold coordination is also supported by another CPMD study which predicted a square pyramidal geometry with an elongated axial water molecule.<sup>18</sup> On the other hand, some quantum mechanical/molecular mechanical (QM/

MM) studies predict a 6-fold coordination and distorted octahedral geometry.<sup>14–16</sup> These discrepancies are not merely the result of differences in methodology but reflect the lack of a robust and computationally inexpensive technique that can perform large-scale simulations of these complex systems for long time scales with models that accurately describe the strong polarization and charge transfer effects.

Copper chloride exists in a plethora of crystal structures and a variety of species in aqueous solution.<sup>22</sup> It is an important species in hydrothermal fluids, and several experimental studies have investigated copper chloride chemistry to better understand metal solubility, transport, and ore deposition mechanisms in geological environments.<sup>23–28</sup> Despite a large number of investigations, the coordination chemistry of aqueous  $\text{CuCl}_2$  is not well resolved. D’Angelo et al. used extended X-ray absorption fine structure (EXAFS) spectroscopy at room temperature to study a 0.1 M  $\text{CuCl}_2$  solution. They proposed a 6-fold Jahn–Teller distorted  $\text{Cu}^{2+}$  coordination with  $\text{Cl}^-$  in the axial position.<sup>29</sup> They found an average  $\text{Cl}^-$  coordination of 0.4 and O (from water) coordination of 5.6 in the first hydration shell of  $\text{Cu}^{2+}$ . At higher chloride concentrations ( $[\text{Cl}^-]/[\text{Cu}^{2+}] = 10$  and 30) the  $\text{Cl}^-$  coordination increases, occupying even the equatorial positions. In contrast, EXAFS studies by Collings et al. could not detect any  $\text{Cu}^{2+}\text{--Cl}^-$  complexation at room temperature in a 0.1 M  $\text{CuCl}_2$  solution.<sup>23</sup> However at very high chloride concentration ( $[\text{Cl}^-]/[\text{Cu}^{2+}] = 52$ ) complexation between the  $\text{Cu}^{2+}$  and  $\text{Cl}^-$  could be detected. Brugger et al. used UV–vis–NIR spectrophotometry to study copper chloride

\* Corresponding author, doren@udel.edu.

<sup>†</sup> University of Delaware.

<sup>‡</sup> The Pennsylvania State University.

<sup>§</sup> California Institute of Technology.

<sup>||</sup> University of Maryland.

complexes.<sup>25</sup> They analyzed the spectra in terms of several Cu(II)–chloro–aqua complexes: distorted octahedral  $[\text{Cu}(\text{OH}_2)_6]^{2+}$ ,  $[\text{CuCl}(\text{OH}_2)_5]^+$ ,  $[\text{CuCl}_2(\text{OH}_2)_4]$ , and (possibly distorted octahedral)  $[\text{CuCl}_3(\text{OH}_2)_3]^-$ , distorted tetrahedral  $[\text{CuCl}_4]^{2-}$ , and dipyramidal trigonal  $[\text{CuCl}_5]^{3-}$ . They conclude that the various determinations of the mean number of first coordination shell chloride ligands were in poor agreement (Figure 11 of ref 25). They note that extraction of the mean ligand number from the EXAFS spectra is difficult due to the small contribution of the apical ligands. Moreover, at higher chloride concentration, multiple replacements of inner hydration shell water by  $\text{Cl}^-$  increase the  $\text{Cl}^-$ – $\text{Cl}^-$  repulsion. This destabilizes the octahedral geometry and transforms it into tetrahedral geometry.<sup>25</sup> Thus an accurate study needs to consider multiple coordination geometries.

The study of aqueous copper complexes is further complicated by the existence of multiple oxidation states of copper,  $\text{Cu}^+$  and  $\text{Cu}^{2+}$ , which have different coordination chemistries. Copper ions predominantly exist as  $\text{Cu}^{2+}$  at room temperature, but the  $\text{Cu}^+$  form is more stable at higher temperatures, making it more relevant to geological environments.<sup>24,27</sup> Recently, Berry et al. suggested a reversible reduction of  $\text{Cu}^{2+}$  to  $\text{Cu}^+$  with increasing temperature and subsequent oxidation of the other species present in the solution.<sup>27</sup> They could deconvolute their X-ray absorption near edge structure (XANES) spectra by a linear combination of  $\text{Cu}^{2+}$  and  $\text{Cu}^+$  spectra suggesting the coexistence of these two oxidation states. Thus, an accurate analysis needs to consider both these oxidation states.

The complex chemistry of  $\text{Cu}^{2+}$  hinders a conclusive interpretation of the experimental observations. Computational methods can supplement experimental observations by direct evaluation of some properties from atomistic simulations. To the best of our knowledge, there are no theoretical investigations of aqueous  $\text{CuCl}_2$ . This is probably because of the lack of a computationally inexpensive technique that can accurately describe the polarization, charge transfer, and Jahn–Teller effects in this system. Ab initio methods that capture the dynamic nature of this system with heterogeneous ligand interactions and multiple oxidation states are computationally very expensive. A force field based method that can describe polarization and charge transfer effects would be better suited for this purpose.

ReaxFF is a bond-order-dependent reactive force field that has been successfully applied to a variety of complex reactive systems.<sup>30–52</sup> Retention of near QM accuracy by ReaxFF at a low computational cost qualifies it for large-scale MD simulations of complex systems. This force field has been developed for a number of metals and metal complexes to describe a variety of metallic properties and metal-catalyzed mechanisms. For example, it has been parametrized for Na and NaH to illustrate the dynamics of  $\text{H}_2$  desorption in NaH particles.<sup>47</sup> During the abstraction process, ReaxFF was able to correctly account for the charge transfer of surface molecular hydrogen and predicted the transformation of the system from ionic to metallic character. This force field has been used to study thermodynamic destabilization of  $\text{MgH}_2$  particles<sup>35</sup> and various dynamic properties in aluminum (Al) and aluminum oxides.<sup>33,43,48</sup>

There are currently ReaxFF descriptions for many transition metals with a variety of applications. For instance, this method precisely characterizes various oxidation states of vanadium(V) and the catalytic activity of vanadium oxide ( $\text{V}_2\text{O}_5$ ) in the oxidative dehydrogenation of methanol to formaldehyde.<sup>45</sup> It has also been parametrized to describe Co, Ni, and Cu atoms and their effects on the catalytic formation of carbon nano-

tubes.<sup>37</sup> It has been used to study the properties of condensed-phase ZnO and its crystal growth.<sup>49</sup> ReaxFF has been developed for other transition metals like Y and  $\text{Zr}^{51}$  and Pt.<sup>42</sup> Finally, a recent work has demonstrated the ability of ReaxFF to capture the complexity of multimetal oxide catalyst systems involving several metals and metalloids like Mo, Te, and Nb.<sup>46</sup>

We selected ReaxFF to model aqueous copper chloride because of its ability to account for the polarization and charge equilibration in metals and metal complexes. Recently, we developed a potential for Cu/O/H by extensive training against a large database of QM energies. This potential successfully reproduces the Jahn–Teller distortion in a  $\text{Cu}^{2+}$ /water system (work in progress). This paper describes the extension of this potential to the Cu/O/H/Cl system. We trained the parameters using QM-based structures and energies of several condensed phase copper chloride clusters as well as Cu/Cl/water clusters generated in MD simulations. We also included hydroxide ions in the QM database to ensure the applicability of this potential to copper chloride in a wide variety of environments and pH values. We present the ability of the potential to describe the structural and dynamic properties of Cl/water and Cu/Cl/water systems and compare them with the experimental observations and theoretical predictions available in the literature. These simulations corroborate the ability of ReaxFF to accurately describe the interactions of  $\text{Cu}^{2+}$  and  $\text{Cl}^-$  ions in water in the presence of strong polarization, charge transfer effects and quantum effects like Jahn–Teller distortion. This potential can be employed as a model to develop computationally affordable tools for large scale simulations of ions in water, condensed phases, and biological environments.

## 2. Computational Methods

**2.1. ReaxFF.** ReaxFF is a bond order dependent reactive force field. The connectivities between the atoms can be modified during a MD simulation allowing spontaneous bond breaking and bond formation. The energy and the forces remain continuous during these processes. Each element is represented by only one atom type in ReaxFF. This facilitates the transferability of the parameters to a different system and avoids the modification of atom types during a chemical reaction. Bond orders  $\text{BO}_{ij}'$  are calculated for each atom pair using the interatomic distance  $r_{ij}$ <sup>30</sup>

$$\text{BO}_{ij}' = \exp\left[p_{\text{bo},1}\left(\frac{r_{ij}}{r_o}\right)^{p_{\text{bo},2}}\right] + \exp\left[p_{\text{bo},3}\left(\frac{r_{ij}^\pi}{r_o}\right)^{p_{\text{bo},4}}\right] + \exp\left[p_{\text{bo},5}\left(\frac{r_{ij}^{\pi\pi}}{r_o}\right)^{p_{\text{bo},6}}\right] \quad (1)$$

where  $(p_{\text{bo},1}$  and  $p_{\text{bo},2}$ ),  $(p_{\text{bo},3}$  and  $p_{\text{bo},4}$ ), and  $(p_{\text{bo},5}$  and  $p_{\text{bo},6}$ ) are the parameters that correspond to the  $\sigma$  bond, the first  $\pi$  bond, and the second  $\pi$  bond, respectively. The value of each of the exponential terms in eq 1 is unity below a particular interatomic distance and negligible at a longer distance. The bond orders  $\text{BO}_{ij}'$  are updated in each MD step. The energy of the system is determined by adding the partial energy contributions like bond energy, valence angle energy, torsion angle energy, etc., and nonbonded van der Waals and Coulomb energies. The bond energy is calculated from the bond order  $\text{BO}_{ij}'$ <sup>30</sup>

$$E_{\text{bond}} = -D_e \text{BO}_{ij} \exp[p_{\text{be},1}(1 - \text{BO}_{ij}^{p_{\text{be},1}})] \quad (2)$$

where  $D_e$  and  $p_{be,1}$  are bond parameters. Upon the dissociation of a bond, the bond order  $BO_{ij}'$  approaches zero making the bond energy term  $E_{\text{bond}}$  disappear (eq 2). The other connectivity related terms like valence angle and torsion angle energy terms are also bond order dependent and they disappear upon bond dissociation. This ensures a smooth transition of the energy and the corresponding force from a bonded system to a nonbonded system.

The nonbonded interactions need to be calculated between every atom pair in order to describe a system with changing connectivity. Thus, the van der Waals energy is calculated between all atom pairs using a distance-corrected Morse potential. A shielded interaction is implemented to avoid the excessive high repulsion between the bonded atom pairs. In a similar fashion, the Coulomb energy is calculated between all atom pairs using a shielded coulomb potential. For each element, the electronegativity, hardness, and shielding parameters are optimized to reproduce the QM derived charges. To account for the polarization effect, the atomic charges are dynamically derived using the electronegativity equalization method (EEM).<sup>53</sup> For further details about the ReaxFF method see refs 30 and 54.

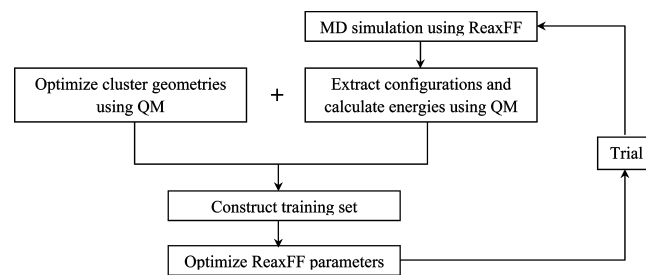
There are some features in ReaxFF that make it a very convenient and useful method to describe reactive systems. In ReaxFF, predefinition of the reactive site or pathways is not required. In a MD simulation, the potential function is capable of administering the chemical reaction in a spontaneous fashion. ReaxFF is computationally much less expensive than QM. However, it can reproduce near QM accuracy in a variety of systems. Thus, this force field is suitable for large-scale dynamic simulations of many reactive systems.

**2.2. Quantum Mechanical Calculations.** The B3LYP<sup>55,56</sup> hybrid DFT method was applied in combination with the 6-311++g(2df,2p) basis set for all cluster quantum mechanical calculations. Several clusters involving copper, chloride, hydroxide, and water were optimized using this QM method. Vibrational frequency analyses were performed to confirm the true minima for each optimized complex. No imaginary frequencies could be detected for the structures optimized in the absence of restraints. For clusters taken from MD simulations, no optimization or frequency analysis was done.

Interaction of Cl with the Cu(111) surface was characterized using periodic DFT calculations. The PBE generalized gradient approximation<sup>57</sup> as implemented in SeqQuest<sup>58</sup> was applied with a Gaussian double- $\zeta$  basis set with polarization functions. Norm conserving pseudopotentials replaced the core electrons in all atoms and a double- $\zeta$  plus polarization Gaussian basis set was used for explicit electrons. A p(2 × 2) cell with three layers of Cu atoms (4 atoms per layer) was used as a two-dimensional periodic model of the Cu(111) surface. The unit cell parameters parallel to the slab were fixed to give the experimental lattice spacing for bulk copper (3.61 Å) within each layer, and the unit cell vector normal to the slab was 21 Å. The Cu atoms in the bottom layer were fixed at their bulk positions for geometry minimization.

**2.3. Molecular Dynamics Simulations. Chloride in Water.** We performed an NVT simulation with a  $[\text{Cl}(\text{H}_2\text{O})_{216}]^-$  in a cubic simulation box of length 18.62 Å. Periodic boundary conditions were applied and the temperature was kept at 300 K with a Berendsen thermostat and a temperature damping constant of 0.1 ps. The time step of the simulation was 0.25 fs. The density was maintained at 1.01 kg/dm<sup>3</sup>. Configurations generated in the first 25 ps of simulation were discarded to allow

## SCHEME 1: The Iterative Scheme for ReaxFF Parameter optimization



for equilibration. Configurations generated in the next 75 ps were considered for the generation of radial distribution function (RDFs).

**Copper Chloride in Water.** An NVT-MD simulation was performed with a  $[\text{CuCl}(\text{H}_2\text{O})_{214}]^+$  system in a cubic box of length 18.62 Å and a time step of 0.25 fs. The temperature was maintained at 300 K with a Berendsen thermostat and periodic boundary conditions were applied. The density of the system was maintained at 1.02 kg/dm<sup>3</sup> throughout the simulation. Configurations generated in the first 75 ps of simulation were discarded, and the next 175 ps of simulation were considered for sampling configurations and analysis.

## 3. Results and Discussion

**3.1. ReaxFF Force Field Parameterization.** To derive a model potential for chloride and copper chloride in water, we extended the ReaxFF potential for Cu/O/H interactions that has been extensively optimized against the QM energies of various copper–water clusters and copper metal/metal oxide/metal hydroxide condensed phases (work in progress). This potential successfully describes  $\text{Cu}^{2+}$  in water as predicted by QM<sup>3</sup> and observed experimentally.<sup>8</sup> New parameters for Cu/Cl/O/H interactions have been added to the previously existing set of Cu/O/H interaction potentials.

We applied an iterative approach for the parametrization of the ReaxFF force field (see Scheme 1).

Two different methods were used to generate configurations:

- We optimized several copper chloride, copper/water/hydroxide, copper/water/chloride, copper/hydroxide, and copper/chloride/water/hydroxide clusters using QM. These configurations and energies were used to generate an initial set of ReaxFF parameters.

- Thereafter, we followed the strategy suggested by Wood et al. by sampling configurations from a classical ReaxFF MD-simulation and refitting the ReaxFF model to QM energies<sup>59</sup> from single-point energy evaluations of structures obtained from MD-simulations with the prior parametrization of the ReaxFF model. This method is computationally efficient because it does not require the derivation of forces from QM. Following this approach we have sampled configurations from MD simulations on chloride, copper/chloride, and copper/chloride/hydroxide in water.

In the end, all of these configurations were combined in one training set. The force field parameters were optimized to reproduce the QM energies of the clusters in the training set. The total error was monitored. The MD simulations were repeated using the optimized set of ReaxFF parameters. The training set was reconstructed with the new configurations extracted from the MD simulations and the parameters were reoptimized. The loop was iterated in this fashion until the error converged and it was not possible to significantly reduce it by

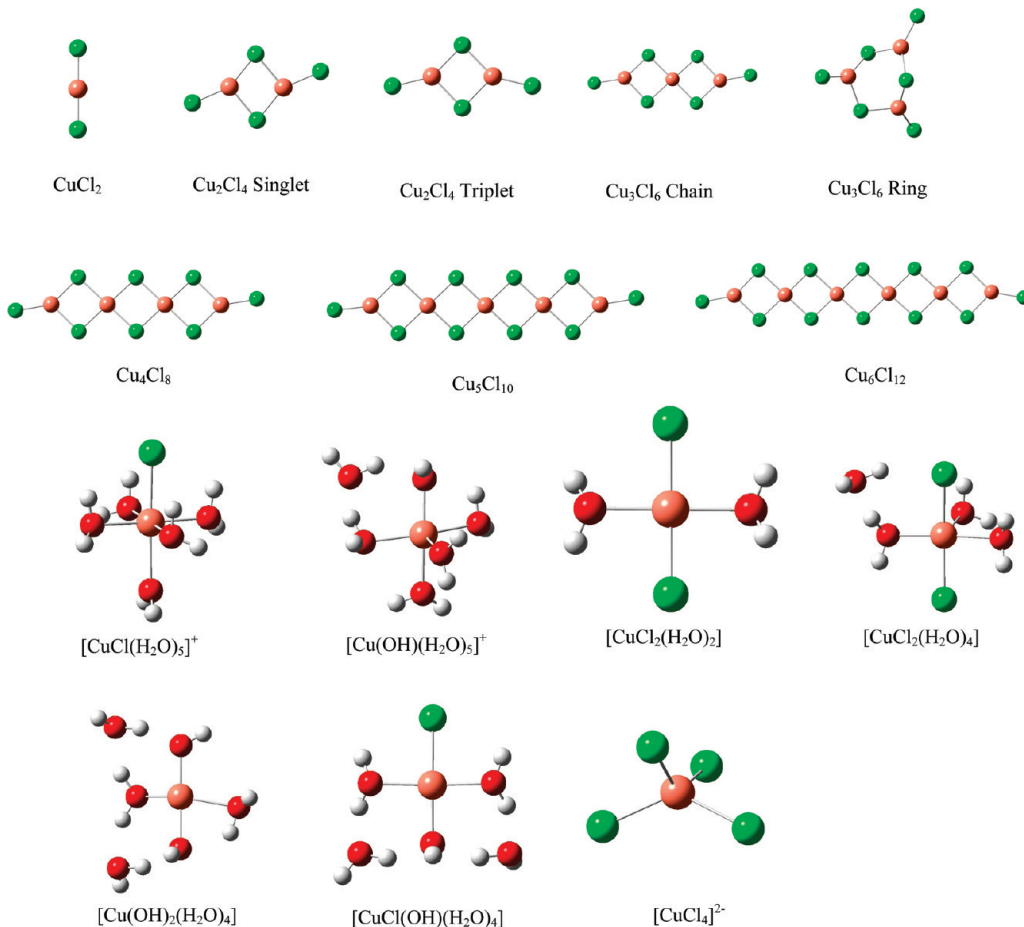


**Figure 1.** QM optimized geometries of several complexes used to develop the initial ReaxFF force field.

a further iteration. A total of five iterations were necessary to reach a convergence by 0.56 kcal/species. The final parameters (see Appendix) were used in the MD simulations on chloride ion and copper chloride in water reported below.

**3.1.1. Copper Chloride Clusters.** We performed geometry optimization on several clusters of copper chloride derived from condensed phase structures (Figure 1). A bridging Cu–Cl–Cu conformation constructs a stable structure which is commonly found in copper chloride complexes (see ref 22 for a comprehensive review of the crystal structures of chlorocuprates). This basic formation can be stacked to form infinite chains with a 4-fold coordination of the copper. Thus, some of these structures are included in the training set. Several other clusters involving chloride, copper, water, and hydroxide are also included in order to ensure that the force field behaves well in the aqueous environment as well as with a variation of pH. Figure 1 shows the QM optimized geometries of the complexes (see Computational Methods section for details). After fitting the parameters, ReaxFF could satisfactorily reproduce the geometries (rmsd = 0.313 Å) and QM energies of these complexes. Table 1 shows the comparison between QM and ReaxFF relative energies of these species.

We have used  $\text{Cu}_2\text{Cl}_4$  as a model to derive the bond dissociation and angle distortion energies relevant to copper chloride.  $\text{Cu}_2\text{Cl}_4$  can be either a singlet or triplet depending on the spin coupling of the d-electrons. ReaxFF is usually parametrized to reproduce the properties of the lowest energy spin state because it does not distinguish between the multiple spin states. According to the QM calculations, the  $\text{Cu}_2\text{Cl}_4$  triplet state was 18.93 kcal/mol lower in energy than the singlet state.

**TABLE 1: QM and ReaxFF Relative Energies of Gas-Phase Copper-Chloride Complexes**

species	QM relative energy (kcal/mol)	ReaxFF relative energy (kcal/mol)
$\frac{1}{2}E(\text{Cu}_2\text{Cl}_4) - E(\text{CuCl}_2)$	-9.46	-28.72
$\frac{1}{2}E(\text{Cu}_2\text{Cl}_4) - \frac{1}{3}E(\text{Cu}_3\text{Cl}_6\text{Chain})$	4.23	5.67
$\frac{1}{2}E(\text{Cu}_2\text{Cl}_4) - \frac{1}{3}E(\text{Cu}_3\text{Cl}_6\text{Ring})$	-0.11	4.59
$\frac{1}{2}E(\text{Cu}_2\text{Cl}_4) - \frac{1}{4}E(\text{Cu}_4\text{Cl}_8)$	6.38	8.27
$\frac{1}{2}E(\text{Cu}_2\text{Cl}_4) - \frac{1}{5}E(\text{Cu}_5\text{Cl}_{10})$	7.64	10.03
$\frac{1}{2}E(\text{Cu}_2\text{Cl}_4) - \frac{1}{6}E(\text{Cu}_6\text{Cl}_{12})$	8.49	11.25
$\frac{1}{2}E(\text{Cu}_3\text{Cl}_6\text{Chain}) - \frac{1}{3}E(\text{Cu}_3\text{Cl}_6\text{Ring})$	-4.33	-1.08
$(E[\text{CuCl}_2(\text{H}_2\text{O})_5]) + E(\text{H}_2\text{O}) - (E[\text{CuCl}(\text{OH})(\text{H}_2\text{O})_4] + E(\text{HCl}))$	-11.34	-25.98
$(E[\text{CuCl}(\text{OH})(\text{H}_2\text{O})_4] + E(\text{H}_2\text{O})) - (E[\text{Cu}(\text{OH})_2(\text{H}_2\text{O})_4] + E(\text{HCl}))$	-25.49	-20.35

Thus we have considered the triplet state to train the force field. Figure 2a demonstrates the Cu–Cl bond dissociation energies and equilibrium bond lengths. The Cu–Cl bond length was held constant by a restraining force while the other coordinates were minimized. ReaxFF satisfactorily reproduces the trend in the QM dissociation energy as well as the equilibrium bond length. Similarly angular restraints were applied to fix a particular angle while minimizing the rest of the molecule. The QM and ReaxFF distortion energies for the  $\angle(\text{Cl}-\text{Cu}-\text{Cl})$  and  $\angle(\text{Cu}-\text{Cl}-\text{Cu})$  are in good agreement (Figure 2b–d).

We also included angle distortion energies of a QM optimized  $[\text{CuCl}(\text{OH})(\text{H}_2\text{O})_4]$  cluster. We initiated the optimization with an octahedral coordination of the  $\text{Cu}^{2+}$  with one  $\text{Cl}^-$ , one  $\text{OH}^-$ , and four  $\text{H}_2\text{O}$  molecules. A nearly planar configuration was obtained at the end of this gas phase optimization (Figure 3). We note that different coordination geometries of this species may be possible in bulk solution. The QM and ReaxFF distortion

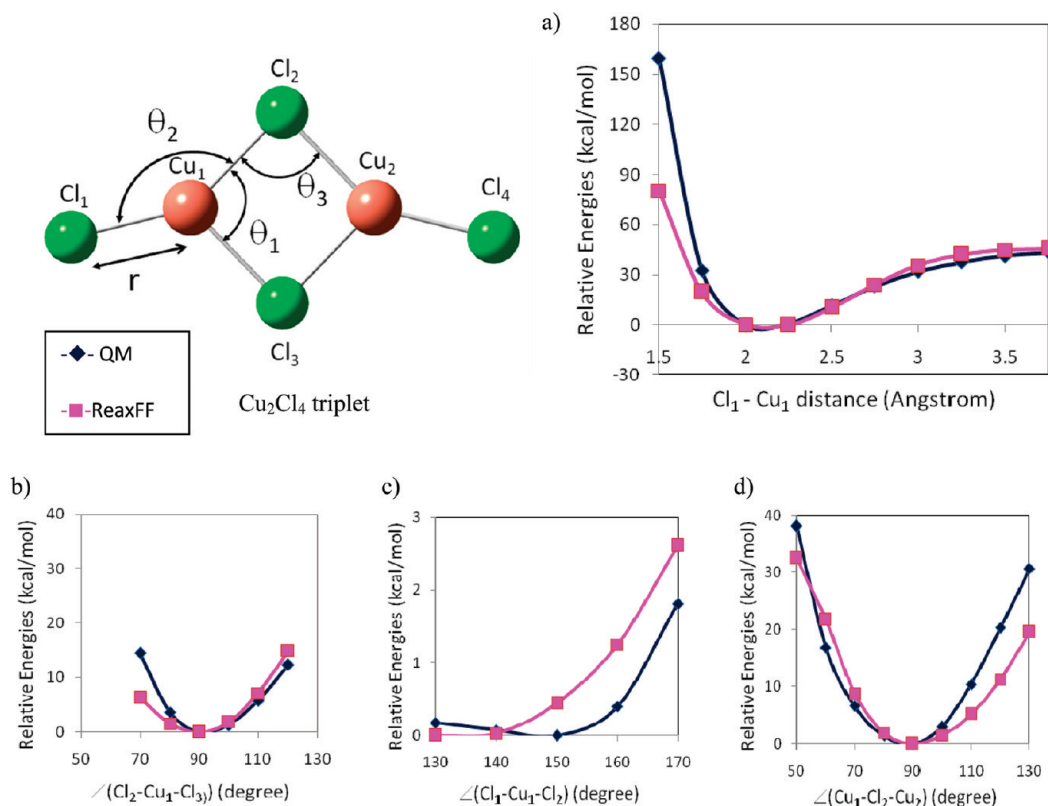


**Figure 2.** Comparison of potentials for  $\text{Cu}_2\text{Cl}_4$  in the triplet state as predicted by QM and the refitted ReaxFF model as a function of (a)  $\text{Cu}-\text{Cl}$  bond distance,  $r$ , and (b)  $\angle(\text{Cl}_2-\text{Cu}_1-\text{Cl}_3)$ , (c)  $\angle(\text{Cl}_1-\text{Cu}_1-\text{Cl}_2)$ , and (d)  $\angle(\text{Cu}_1-\text{Cl}_2-\text{Cu}_2)$  angle distortions.

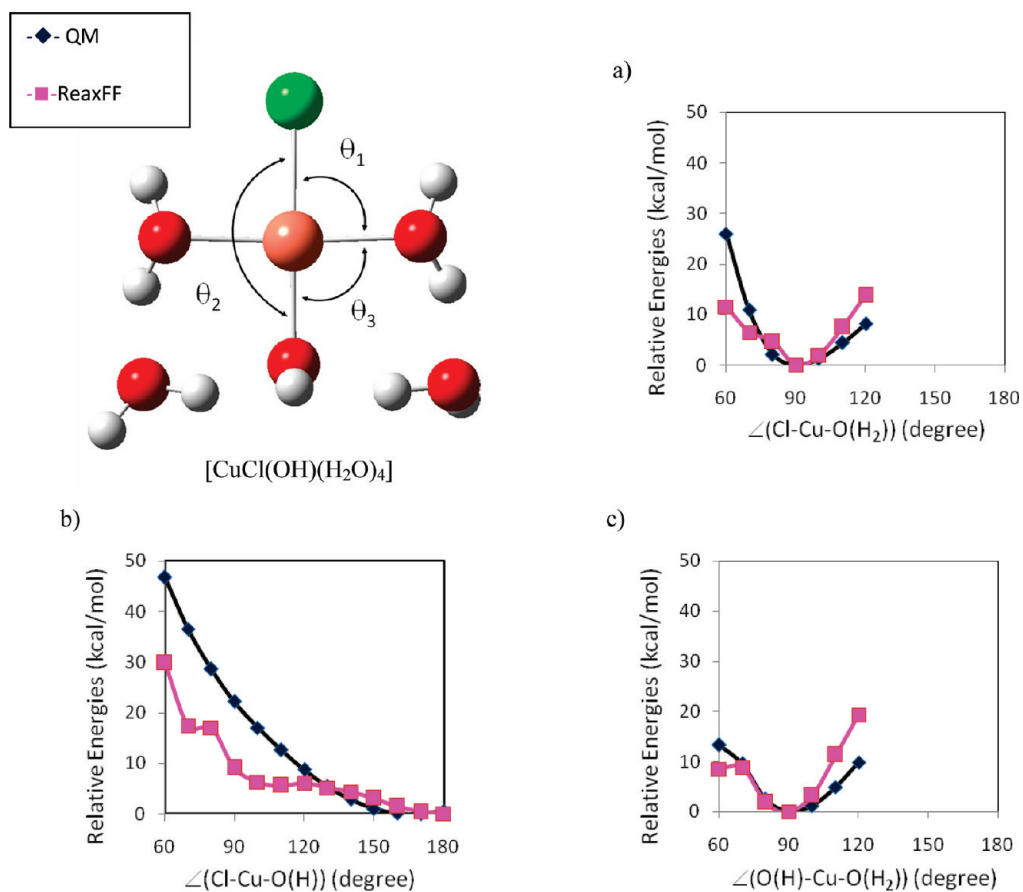


**Figure 3.** Comparison of potentials for  $[\text{CuCl}(\text{OH})(\text{H}_2\text{O})_4]$  cluster as predicted by QM and the refitted ReaxFF model as a function of (a)  $\angle(\text{Cl}-\text{Cu}-\text{O}(\text{H}_2))$ , (b)  $\angle(\text{Cl}-\text{Cu}-\text{O}(\text{H}))$ , and (c)  $\angle(\text{O}(\text{H})-\text{Cu}-\text{O}(\text{H}_2))$  angle dissociations.

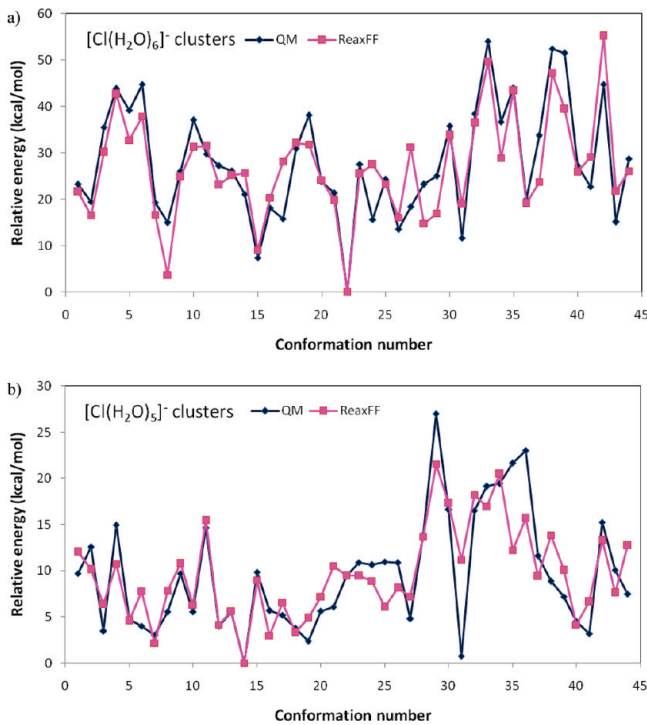


**Figure 4.** Comparison of QM and ReaxFF relative energies of  $[\text{Cl}(\text{H}_2\text{O})_6]^-$  clusters (a) extracted from an MD simulation using the initial parameters of ReaxFF. (b) QM and ReaxFF relative energies of  $[\text{Cl}(\text{H}_2\text{O})_5]^-$  clusters extracted from a new MD simulation using the final parameters of ReaxFF.

energies for various angles in the cluster agree well, particularly near the minima (Figure 3). The ability of ReaxFF to successfully reproduce the QM energies and configurations for these systems provides us with a tool to describe copper chloride in the presence of hydroxide ions.

**3.1.2. Chloride Ion in Water.** A NVT MD simulation was performed with a  $\text{Cl}^-$  and 216 water molecules at 300 K for 125 ps using the initial set of ReaxFF parameters. Several  $[\text{Cl}(\text{H}_2\text{O})_6]^-$  clusters were extracted in regular intervals from the simulation, and the ReaxFF parameters were reoptimized against the QM single point energies. After the reoptimization, the QM and ReaxFF single point energies in the training set agreed with an average unsigned error of 4.76 kcal/mol (Figure 4a). Among the 44 clusters, cluster numbers 8, 17, 24, 27, and 39 produced the largest errors. A direct visualization of these clusters did not detect any special structural features that were absent in the other clusters. Thus, these larger errors seem to belong to the random errors of the ensemble. Following this, we performed another NVT MD simulation using the refitted ReaxFF model. The new set of parameters produced a 5-fold coordination of  $\text{Cl}^-$ . We extracted several  $[\text{Cl}(\text{H}_2\text{O})_5]^-$  clusters from the simulation for single point energy calculations. Again the QM and ReaxFF energies were in accord (Figure 4b), with an average unsigned error of 2.52 kcal/mol. This confirmed that the ReaxFF force field parameters were transferable to a set of new configurations generated by the optimized potential. We note that, among the 44 clusters, cluster numbers 29, 31, 35, 36, and 44 produced the largest errors. A direct visualization of these clusters revealed that the central  $\text{Cl}^-$  in all of these clusters possessed an effective 4-fold coordination. The fifth water molecule was relatively farther away interacting indirectly with the  $\text{Cl}^-$  through another water molecule in the first hydration shell. Although the  $\text{Cl}^-$  had an overall 5-fold coordination, these clusters were among the few that represented

the under coordinated 4-fold states. The relatively larger errors for these cases suggest that, even though the ReaxFF parameters obtained from the  $[\text{Cl}(\text{H}_2\text{O})_6]^-$  clusters were transferable to the  $[\text{Cl}(\text{H}_2\text{O})_5]^-$  clusters, the accuracy is expected to decrease with larger deviations of the coordination number. As a general rule, ReaxFF parameters are transferable to a new system with a similar chemical environment. A larger deviation in the electrostatic forces, charge transfer, coordination number, etc., normally restrains the transferability of the parameters.

**3.1.3. Copper Chloride and Hydroxide in Water.** We performed three NVT MD simulations with  $[\text{CuCl}(\text{H}_2\text{O})_{214}]^+$ ,  $[\text{CuCl}(\text{OH})(\text{H}_2\text{O})_{213}]$ , and  $[\text{CuCl}(\text{OH})_2(\text{H}_2\text{O})_{212}]^-$  unit cells at 300 K for 125 ps using the initial set of ReaxFF parameters. The first simulation was started with a  $\text{Cl}^-$  placed in the first hydration shell of a  $\text{Cu}^{2+}$ . The total charge of the system was +1. The  $\text{Cl}^-$  remained in the first hydration shell during the entire simulation. We obtained the initial configuration of the second simulation from the final configuration of the first simulation. We transformed a water molecule residing a few angstroms from the  $\text{Cu}^{2+}$  into  $\text{OH}^-$  by removing a proton from it. The total charge of the system was changed to zero and the second simulation was initiated. During the simulation the  $\text{OH}^-$  migrated to the first hydration shell of the  $\text{Cu}^{2+}$ . At the end of the second simulation, we modified another water molecule residing a few angstroms from the  $\text{Cu}^{2+}$  into  $\text{OH}^-$ . The total charge of the system was changed to -1, and the third simulation was initiated. The second  $\text{OH}^-$  also migrated to the first hydration shell of the  $\text{Cu}^{2+}$ . Several  $[\text{CuCl}(\text{H}_2\text{O})_5]^+$ ,  $[\text{CuCl}(\text{OH})(\text{H}_2\text{O})_4]$ , and  $[\text{CuCl}(\text{OH})_2(\text{H}_2\text{O})_3]^-$  clusters were extracted at regular intervals from the three simulations, and QM-single point energies were calculated for these clusters. The final parametrization of the force field produced reasonable agreement between the QM and ReaxFF single point energies of the clusters (Figure 5) with average unsigned errors of 9.51, 10.62, and 12.19 kcal/mol for the three simulations respectively.

The analyses of these errors provide a few insights about the applicability of ReaxFF. In general, the large differences between QM and ReaxFF energies in these cases appear to reflect the number of different interacting species like  $\text{Cu}^{2+}$ ,  $\text{Cl}^-$ ,  $\text{OH}^-$ , and  $\text{H}_2\text{O}$ . We note that the errors may be cumulative of the errors in the individual potentials. The force field parameters were optimized with a focus on the  $[\text{CuCl}(\text{H}_2\text{O})_5]^+$  system in the absence of any  $\text{OH}^-$ . However, the addition of an extra  $\text{OH}^-$  in the consecutive simulations resulted in a deviation from this system. This is reflected by the gradual increment in the average unsigned error. We note that QM and ReaxFF use different methods to calculate charge transfer and polarizations which play dominating roles in these systems with multiple ligands of miscellaneous types. Thus, the ReaxFF parameters that govern the charge distribution and electrostatic forces in the system inevitably restrain the highest accuracy that can be achieved by ReaxFF. For all the three case, the lowest energy cluster was successfully identified by both ReaxFF and QM. Relatively higher discrepancies were observed for the high energy clusters. Usually, a force field is parametrized with an aim to reproduce the QM geometries and energies of the lowest energy species. This enables the force field to accurately describe the statistically important conformations near the minimum. Accordingly, a major part of our ReaxFF training set consisted of the optimized lowest energy conformations. Thus, it is not surprising that the optimized parameters described the lowest energy conformations better than the higher energy conformations. We also note that, as compared to ReaxFF, QM seems to overestimate the energy differences between the clusters in all

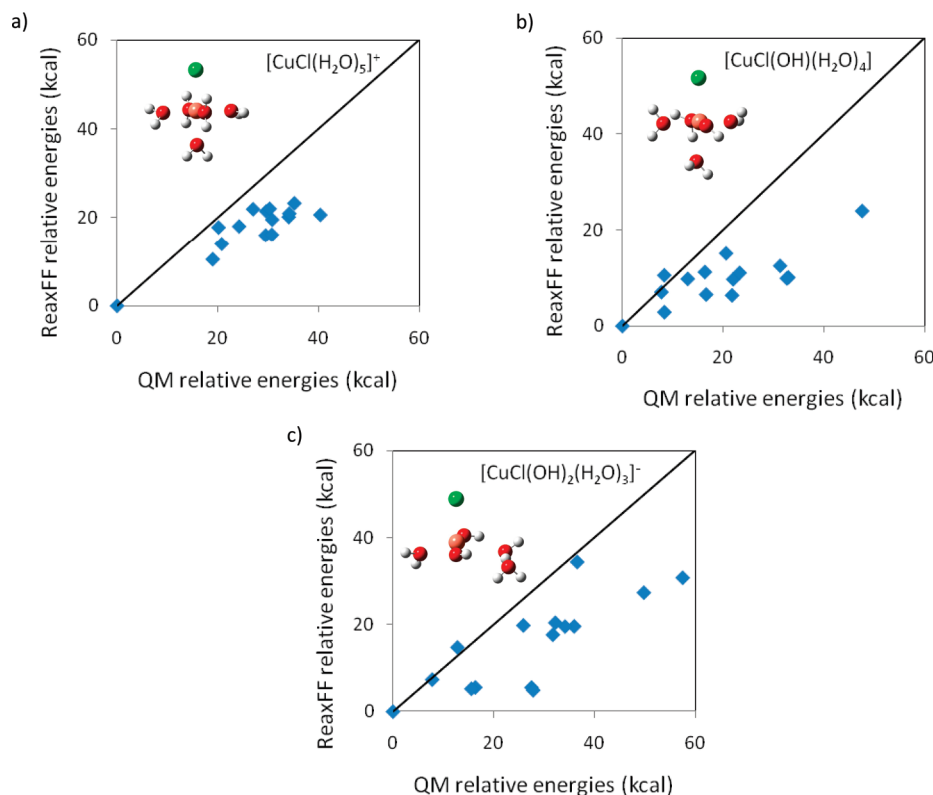


**Figure 5.** Comparison of QM and ReaxFF single point energies of (a)  $[\text{CuCl}(\text{H}_2\text{O})_5]^+$  clusters, (b)  $[\text{CuCl}(\text{OH})(\text{H}_2\text{O})_4]$  clusters, and (c)  $[\text{CuCl}(\text{OH})_2(\text{H}_2\text{O})_3]^-$  clusters extracted from MD simulations.

three cases. This is due to the fact that the clusters were sampled from a MD simulation with ReaxFF energy description. The sample clusters that were extracted at equilibrium were close to the ReaxFF energy minima. However, the ReaxFF and QM potential energy surfaces and minima do not match exactly. Consequently, the sample clusters often deviate from the QM energy minima slightly. Now, due to the curvature of an energy minimum, the clusters that are farther apart from the minimum will have larger energy differences between them as compared to the clusters close to the minimum. This is probably the reason for the overestimation of the QM energy differences of the cluster.

**3.1.4. Cl Adsorption on the Cu[111] Surface.** The adsorption of Cl on the Cu[111] surface has been investigated by both experimental<sup>60–62</sup> and theoretical<sup>63</sup> methods. In order to verify the ability of the force field to correctly estimate the adsorption characteristics, we have constructed a three layer two-dimensional periodic Cu(111) slab using 12 Cu atoms. We computed the potential energy surface for Cl desorption from a face-centered cubic (fcc) site on Cu(111) (the most stable site). During the geometry optimizations the position of the Cl atom was fixed at various distances relative to the bottom layer of Cu atoms (which were also fixed), while the top and middle layers of Cu atoms were allowed to relax. The QM and ReaxFF relative energies agree along the entire reaction path (Figure 6a).

We considered Cl binding to various high symmetry sites on and in the Cu(111) surface. The fcc site is a local minimum for Cl, while constraints are required to hold Cl at the bridge and top sites. We also considered the case of Cl substituted for a Cu atom in the surface, creating a Cu adatom, as well as the case of an interstitial Cl atom directly below the Cu surface layer. The systems were optimized with necessary restraints to keep the Cl in the binding site of interest. The QM and ReaxFF

relative energies for these sites are congruous (Figure 6b). Both ReaxFF and QM could correctly recognize the fcc site as the strongest binding site followed by the bridge and the atop site. This agrees with the previous DFT study<sup>63</sup> (Table 2).

**3.1.5. HCl Dissociation in Water Clusters.** As a strong acid, HCl dissociates into  $\text{Cl}^-$  and  $\text{H}^+$  in bulk water. Several studies have predicted that at least four or five  $\text{H}_2\text{O}$  molecules are necessary for the ionic dissociation of HCl in a water cluster.<sup>64–67</sup> A recent study investigated an aggregation-induced dissociation of HCl in aqueous droplet formed in superfluid helium cluster at  $T = 0.37 \text{ K}$ .<sup>68</sup> Analysis of infrared laser spectra and ab initio simulations demonstrated the dissociation of HCl with the aggregation of a fourth water molecule in the droplet. We performed a preliminary study to distinguish the associated and dissociated states of HCl interacting with one  $\text{H}_2\text{O}$  and a cluster of several  $\text{H}_2\text{O}$  molecules. The H–Cl distance was fixed at different values during DFT optimizations of the clusters, and the results were included in the database used to optimize ReaxFF parameters. Both QM and ReaxFF energies predict that HCl prefers an associated form with one  $\text{H}_2\text{O}$ , but it prefers the dissociated form with five or seven  $\text{H}_2\text{O}$  molecules (Figure 7). This agrees with the previous studies mentioned above.<sup>64–68</sup>

**3.2. Molecular Dynamics Simulation of Chloride Ion in Water.** To further validate the optimized ReaxFF potential for chloride ion, it has been tested in a NVT MD simulation of  $[\text{Cl}(\text{H}_2\text{O})_{216}]^-$  system (see Computational Methods section for details). The  $\text{Cl}^-$  interaction with bulk water has been characterized by the radial distribution functions (RDFs) of Cl–H and Cl–O. The results obtained from the simulations agree with the theoretical and experimental data available in the literature as summarized by Tongraar and Rode (Table 2 of ref 69). Our simulated Cl–H RDF had a sharp first peak at 2.04 Å and a relatively broad second peak at 3.45 Å (Figure 8a). The first peak corresponds to the hydrogen atoms of water molecules

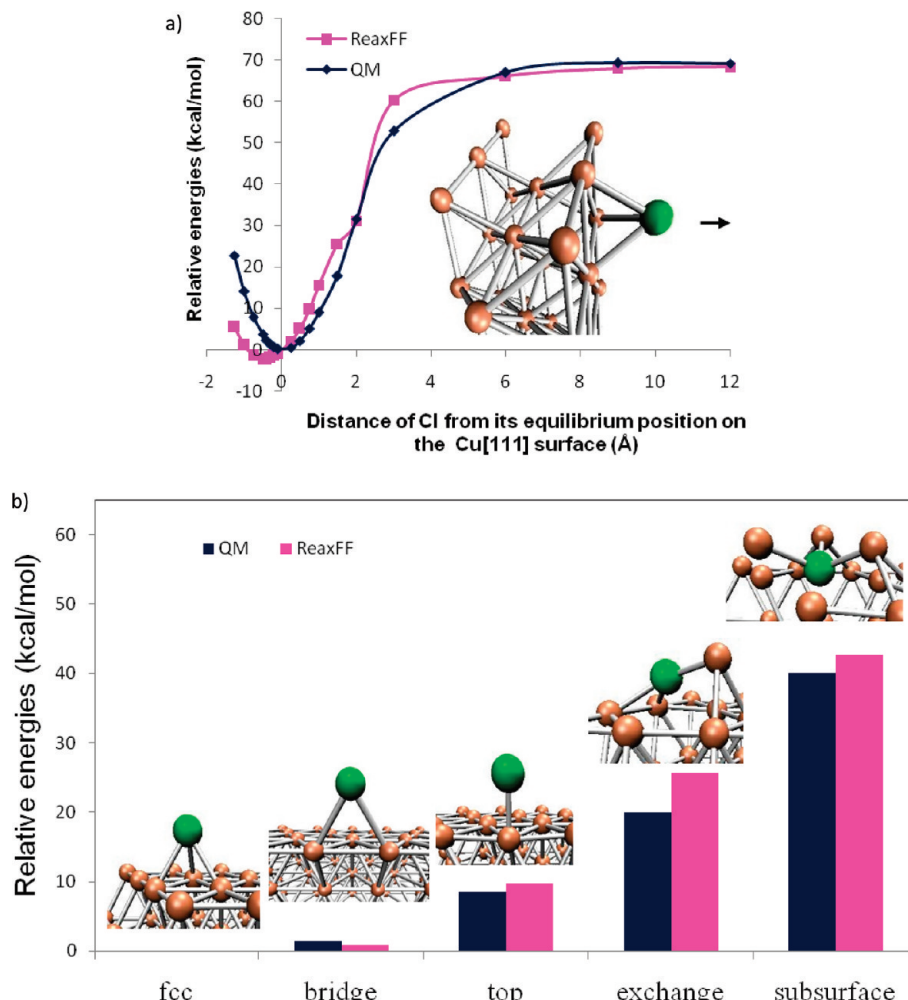


**Figure 6.** Cl on Cu[111] surface: (a) Comparison of QM and ReaxFF dissociation energies of Cl from Cu[111] surface (fcc-site). (b) Comparison of QM and ReaxFF binding energies of Cl at the Cu[111] fcc, bridge, top, exchange and subsurface sites. Energies are relative to the system with Cl bound to the fcc-Cu[111] site.

**TABLE 2: QM and ReaxFF Relative Energies of Different Cl Binding Sites on Cu[111] Surface**

binding site	ReaxFF relative energy (kcal/mol) (this work)	QM relative energy (kcal/mol) (this work)	QM relative energy (kcal/mol) (ref 63) <sup>a</sup>
fcc	0	0	0
bridge	0.94	1.43	1.74–2.00
top	9.79	8.51	10.38–10.64

<sup>a</sup> DFT results from Table 6 of ref 63.

closest to the anion. Neutron diffraction experiments reported a range of 2.22–2.29 Å for the first peak position of the Cl–H RDF.<sup>70</sup> A recent neutron diffraction study predicted a slightly shorter value of 2.14 ± 0.02 Å.<sup>71</sup> Our calculated value of 2.04 Å is reasonably close to these studies. The coordination number of hydrogen was 4.9, as determined by integration of the RDF ( $n(r)$ ) to the location of the first minimum of the RDF. On the other hand the first peak of the Cl–O RDF is at 3.07 Å (Figure 8b) and the coordination number of oxygen was 4.91 as indicated by integration of  $n(r)$  to the location of the first minimum of the RDF. The experimental range of values for the first peak position of the Cl–O RDF is 3.1–3.3 Å while theoretical values are in the range 3.15–3.9 Å.<sup>69</sup> Our calculated value of 3.07 Å falls reasonably close to these ranges. The  $n(r)$  of both Cl–H and Cl–O suggest 5-fold coordination of the water molecules around the chloride ion. The RDFs have nonzero values between the first and the second peak for both

Cl–H and Cl–O distributions. This suggests some exchange of water molecules between the bulk and the first solvation shell of the chloride ion during the simulation. To test whether the appearance of 5-fold coordination might be biased by the initial configuration, we also initiated a MD-simulation starting from a 6-fold coordination. However, this configuration transformed into a 5-fold coordinated species after 6.5 ps.

In ReaxFF, the total charge of the system is distributed over all the atoms in the simulation box according to the electronegativity equalization method (EEM) scheme.<sup>53</sup> Thus charge transfer is allowed between the chloride ion and the water molecules or among the water molecules. We observe significant charge transfer from the chloride ion to the water molecules. The average value of the chloride ion charge was −0.71 e.

Despite the available experimental and theoretical studies, the coordination number of chloride ion in aqueous solution is not well determined. Experimental observations have found a broad range of values: 4–9 with a strongly preferred value of 6.<sup>69,70,72</sup> Computational studies also predict a broad range, 5.1–8.4. The nonpolarizable TIP4P or SPC/E water models lead to the higher values in this range.<sup>69</sup> A fixed charge of −1 on the chloride ion induces strong short-range interactions with the closest water molecules and results in overcoordination. More recent studies incorporating charge transfer and polarization effects yield lower coordination numbers. Tongraar and Rode have applied a combined QM/MM MD simulation to aqueous

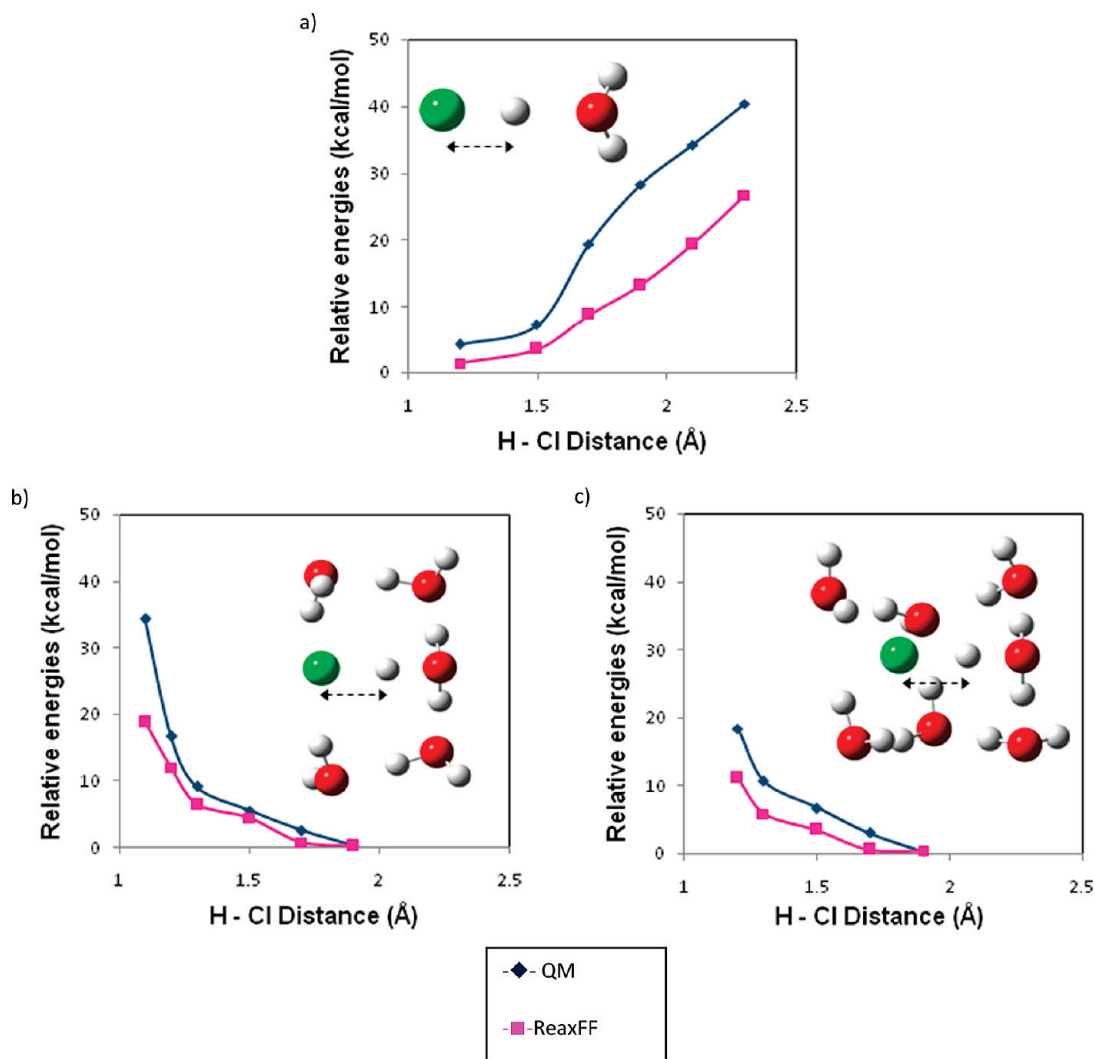


**Figure 7.** QM and ReaxFF energies of  $[HCl(H_2O)]$ ,  $[HCl(H_2O)_5]$ , and  $[HCl(H_2O)_7]$  clusters at fixed H–Cl distances. The energies suggest that HCl prefers to be in the associated form with one  $H_2O$  but in the dissociated form with five or seven  $H_2O$  molecules.

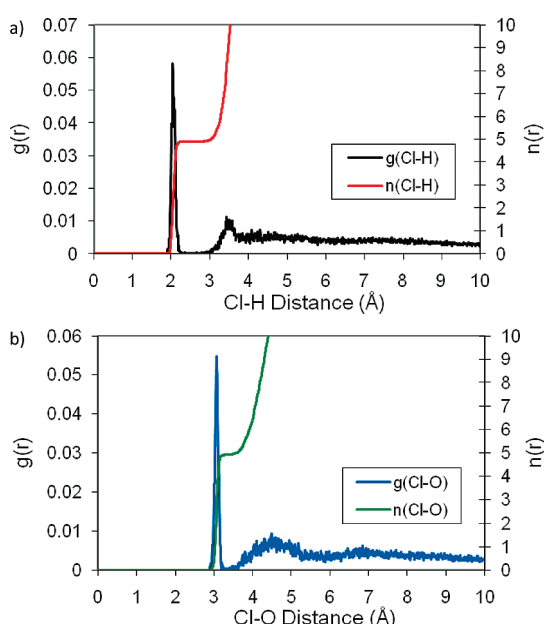


**Figure 8.** (a) Cl–H and (b) Cl–O radial distribution functions and integrals as obtained from the ReaxFF MD simulation on a  $[Cl(H_2O)_{216}]^-$  system at  $T = 300$  K.

chloride ion, allowing free charge transfer from the anion to the water molecules in the first hydration shell.<sup>69</sup> The chloride ion acquired a charge of  $-0.89$  e and a coordination number of 5.6, which is lower than most of the previous theoretical values. Heuft and Meijer have used a CPMD simulation to predict an average chloride coordination number of 5.0 and 5.6 for Cl–H and Cl–O, respectively.<sup>73</sup> Recently, Laage and Hynes used a polarizable and flexible Amoeba force field to simulate the rotational dynamics of water molecules in the first hydration shell of the chloride ion.<sup>74</sup> They found that at equilibrium five hydrogen bonds are accepted by  $Cl^-$ . Thus the 5-fold coordination of the chloride predicted by ReaxFF simulation is in agreement with these computational studies that account for polarization and charge transfer.

An analysis of the angular distribution of the first hydration shell water molecules around the chloride ion facilitated the determination of its coordination geometry. The  $\angle(O \cdots Cl \cdots O)$  angular distribution was calculated from the  $[Cl(H_2O)_5]^-$  clusters extracted from the MD simulation (Figure 9a). This demonstrates the distribution of the five closest water molecules around the chloride ion. The angles were distributed over a wide range, from about  $40^\circ$  to  $180^\circ$  with a peak at  $85^\circ$ . This implies that the coordination geometry of solvated chloride ion is not very rigid. It appears to be rather irregular, which does not belong to a specific type of geometry. Direct visualization of the

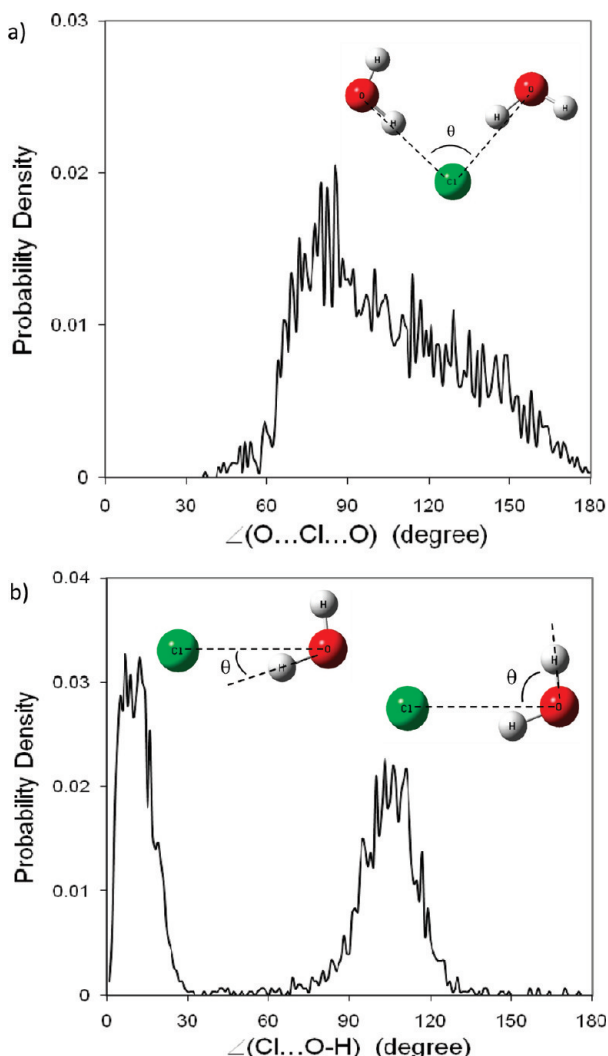


**Figure 9.** (a)  $\angle(O\cdots Cl\cdots O)$  and (b)  $\angle(Cl\cdots O\cdots H)$  angular distribution considering the  $[Cl(H_2O)_5]^-$  clusters obtained from the ReaxFF MD simulation on a  $[Cl(H_2O)_{216}]^-$  system at  $T = 300$  K.

configurations shows continuous variation of chloride ion coordination geometry during the simulation. In their simulation with the polarizable Amoeba forcefield, Laage and Hynes<sup>74</sup> also concluded that the first hydration shell of the anion was very labile. However, this contradicts previous studies that suggested a rigid conformation,<sup>73,75,76</sup> and more experimental investigation may be necessary to resolve this problem.

The orientation of the first hydration shell water molecules with respect to the chloride ion is of particular interest. The  $\angle(Cl\cdots O\cdots H)$  angular distribution was calculated using the  $[Cl(H_2O)_5]^-$  clusters extracted from the MD simulation (Figure 9b). The peaks between  $0^\circ$  and  $30^\circ$  denote the  $\angle(Cl\cdots O\cdots H)$  angles with the hydrogen atom directly interacting with the chloride ion. The absence of any peak at  $0^\circ$  was also observed by Tongraar and Rode in their QM/MM simulation of the aqueous chloride ion (Figure 1 of ref 77). This aversion of a perfect alignment is not a consequence of physical interactions between atoms. The angles are uniformly distributed in a spherical coordinate system ( $r, \theta, \phi$ ). The calculated probability distribution corresponds to the one-dimensional angular distribution ( $\theta$ ) that is reduced from a two-dimensional angular distribution ( $\theta, \phi$ ). This results in a scaling of the actual probability distribution by  $\sin(\theta)$ . There is no peak at  $0^\circ$  because  $\sin(\theta)$  has a value of zero at this point. The peaks between  $70^\circ$

and  $130^\circ$  correspond to the hydrogen atoms farther from the chloride ion. There were very few configurations with  $\angle(Cl\cdots O\cdots H)$  angles falling between these two regions. These observations indicated a strong alignment of the first hydration shell water molecules such that a single hydrogen is oriented toward the chloride ion. QM/MM simulation of aqueous chloride ion by Tongraar and Rode predicted that there are also bridging water molecules in which both hydrogen atoms simultaneously interact with the chloride ion.<sup>69,77</sup> Although our other results are comparable to these studies, we did not observe bridging structures. To the best of our knowledge, there is no experimental evidence for the existence of this structure.

**3.3. Molecular Dynamics Simulation of Copper Chloride in Water.** We have further tested the optimized ReaxFF potential by performing a MD simulation of aqueous copper chloride. Aqueous copper chloride can exist in multiple forms depending on the ratio  $[Cu^{2+}]/[Cl^-]$ . With increasing  $Cl^-$  concentration, one or more  $Cl^-$  gradually replace the water molecules in the inner sphere of  $Cu^{2+}$  forming species like  $CuCl^+$ ,  $CuCl_2$ ,  $CuCl_3^-$ ,  $CuCl_4^{2-}$ , etc.<sup>22,25,78</sup> We have specifically focused our work on a highly dilute  $CuCl^+$  solution. D'Angelo et al. performed X-ray absorption spectroscopy to detect Jahn-Teller distorted octahedral  $Cu^{2+}$  coordination in 0.1 M  $CuCl_2$  solution with  $Cl^-$  interacting in the axial position.<sup>29</sup> They suggested that, on average, 0.4  $Cl^-$  occupied the axial position and 5.6 water molecules occupied the other positions completing the octahedral coordination. The partial occupation of the  $Cl^-$  in the  $Cu^{2+}$  hydration sphere suggests that the free energy of the  $CuCl^+$  species would be comparable to the free energy of a hydrated  $Cu^{2+}$  with a  $Cl^-$  placed in the bulk water.

To study the  $Cu/Cl$  water system, a NVT MD simulation was started with  $Cl^-$  placed 2.19 Å away from  $Cu^{2+}$  with only two directly interacting water molecules, surrounded by 212 other water molecules. The  $Cl^-$  stayed in the first hydration shell of  $Cu^{2+}$  throughout the entire simulation time. After 4.25 ps of simulation a third water molecule moved into the first hydration sphere of  $Cu^{2+}$  making it 4-fold coordinated. This was followed by a fourth water molecule after another 16.25 ps of simulation time. Finally,  $Cu^{2+}$  acquired a 6-fold coordination with one  $Cl^-$  and five water molecules after another 16.5 ps of simulation. The  $Cu^{2+}$  coordination number remained unchanged for the rest of the 250 ps simulation.

We analyzed the RDFs to characterize the aqueous  $Cu^{2+}$ - $Cl^-$  interaction and to assess the effect of the counterion on the hydration sphere of each ion. The  $Cu-Cl$  RDF has a sharp peak at 2.42 Å and has nonzero values only between 2.24 and 2.71 Å (Figure 10a), suggesting a strong association between the ions. The  $Cl-H$  RDF has a sharp first peak at 2.10 Å and a relatively broad peak at 3.50 Å, with nonzero values between them (Figure 10b). These peak positions are comparable to the peak positions observed in the  $[Cl(H_2O)_{216}]^-$  simulation (Figure 8a), though the presence of the  $Cu^{2+}$  reduces the peak area. An integration of the  $Cl-H$  RDF to the first minimum (2.28 Å) shows that the hydrogen coordination number for chloride is 2.83. Accounting for the  $Cu^{2+}$ , this implies a total  $Cl^-$  coordination number of 3.83. This 4-fold coordination can be compared to the 5-fold coordination observed in the  $[Cl(H_2O)_{216}]^-$  simulation. A direct visualization of the clusters using VMD<sup>79</sup> software also revealed a dominating 4-fold coordination.

The  $Cu-O$  RDF has a sharp peak at 1.97 Å and a broader peak at 4.22 Å (Figure 10c). The RDF is zero between 2.47 Å and the start of the second peak (3.45 Å). This indicates that exchange of water molecules between the first and second hydration shell is rare. Integration over the first  $Cu^{2+}$  coordina-

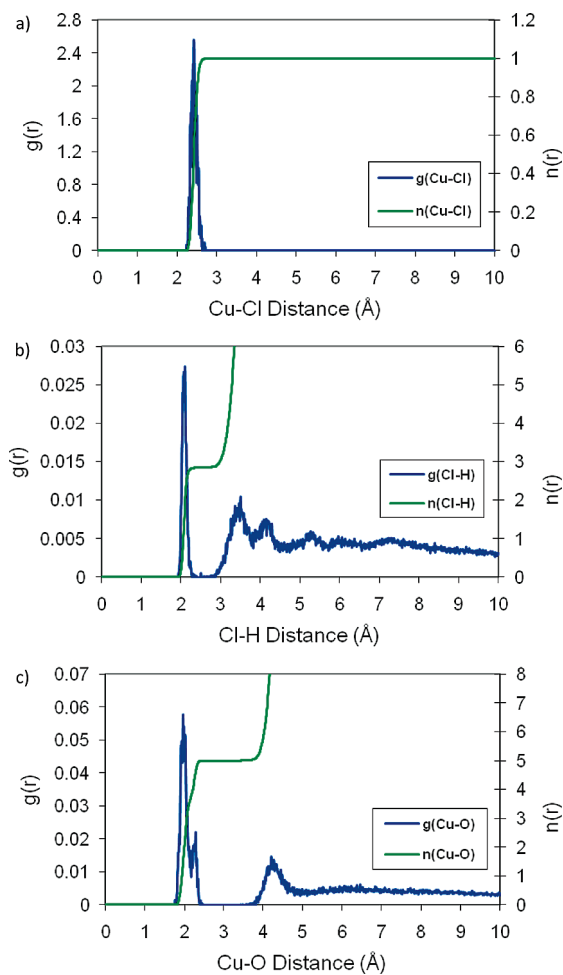


**Figure 10.** (a) Cu–Cl, (b) Cl–H, and (c) Cu–O radial distribution functions and integrals as obtained from the ReaxFF MD simulation on a  $[\text{CuCl}(\text{H}_2\text{O})_{214}]^+$  system at  $T = 300$  K.

tion shell yields five water molecules. Accounting for the  $\text{Cl}^-$ , this implies a 6-fold coordinated  $\text{Cu}^{2+}$  ion. This is identical to the 6-fold  $\text{Cu}^{2+}$ –water coordination observed in a previous ReaxFF simulation study (work in progress). Thus, while the presence of  $\text{Cu}^{2+}$  reduces the coordination number of  $\text{Cl}^-$  by 1, the presence of  $\text{Cl}^-$  does not alter the coordination number of  $\text{Cu}^{2+}$ .

Direct visualizations of  $[\text{CuCl}(\text{H}_2\text{O})_5]^+$  clusters extracted from the MD simulation revealed a 6-fold octahedral  $\text{Cu}^{2+}$  coordination, comparable to the QM optimized  $[\text{CuCl}(\text{H}_2\text{O})_5]^+$  cluster in the gas phase (Figure 1). Figure 11 shows the  $\angle(\text{Cl}\cdots\text{Cu}\cdots\text{O})$  and  $\angle(\text{O}\cdots\text{Cu}\cdots\text{O})$  angular distribution functions constructed from these clusters. Two peaks near  $90^\circ$  and  $175^\circ$  appear in both distributions, consistent with octahedral  $\text{Cu}^{2+}$  coordination. The peaks are sharp and the distribution is zero at intermediate angles, suggesting a rigid conformation of the first hydration shell of  $\text{Cu}^{2+}$ . This is in agreement with the rigid  $\text{O}_{\text{eq}}$ – $\text{Cu}$ – $\text{O}_{\text{eq}}$  angles observed by D’Angelo and co-workers where  $\text{O}_{\text{eq}}$  is an oxygen atom in an equatorial water molecule.<sup>29</sup> The peak positions and rigidity of the hydrated  $\text{CuCl}^+$  species in our simulation are comparable to those of the hydrated  $\text{Cu}^{2+}$  species studied in a previous ReaxFF simulation (work in progress) and QM/MM simulations.<sup>14,16</sup> The  $\text{Cl}^-$  seems to replace a water molecule from the first hydration shell of  $\text{Cu}^{2+}$  without noticeably altering its coordination geometry.

The first peak of the Cu–O RDF has a shoulder, indicating that one or more water molecules coordinate  $\text{Cu}^{2+}$  at a longer

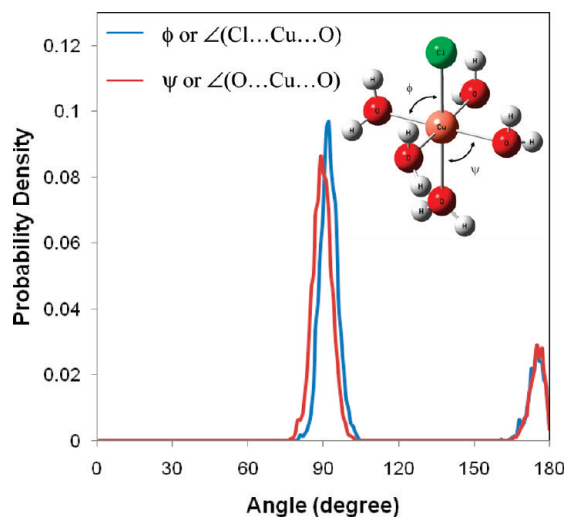


**Figure 11.**  $\angle(\text{Cl}\cdots\text{Cu}\cdots\text{O})$  and  $\angle(\text{O}\cdots\text{Cu}\cdots\text{O})$  angular distributions considering the  $[\text{CuCl}(\text{H}_2\text{O})_5]^+$  clusters obtained from the ReaxFF MD simulation on a  $[\text{CuCl}(\text{H}_2\text{O})_{214}]^+$  system at  $T = 300$  K.

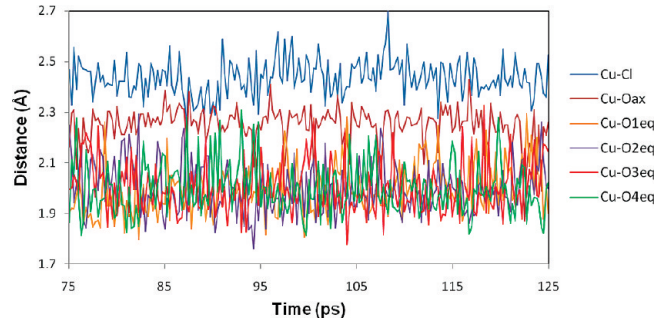


**Figure 12.** Time evolutions of Cu–Cl, Cu–O<sub>ax</sub>, Cu–O1<sub>eq</sub>, Cu–O2<sub>eq</sub>, Cu–O3<sub>eq</sub>, and Cu–O4<sub>eq</sub> bond lengths in the  $[\text{CuCl}(\text{H}_2\text{O})_5]^+$  cluster extracted from the ReaxFF MD simulation on a  $[\text{CuCl}(\text{H}_2\text{O})_{214}]^+$  system at  $T = 300$  K. Results from 75 to 125 ps simulation time are shown.

distance. A direct visualization of the  $[\text{CuCl}(\text{H}_2\text{O})_5]^+$  clusters taken from the simulation, reveals that the axial oxygen atom ( $\text{O}_{\text{ax}}$ , opposite the  $\text{Cl}^-$ ) is farther from  $\text{Cu}^{2+}$  than the equatorial oxygen atoms ( $\text{O}_{\text{eq}}$ ). This is similar to the geometry of the QM optimized gas phase  $[\text{CuCl}(\text{H}_2\text{O})_5]^+$  cluster (Figure 1) with a  $\text{Cu}^{2+}$ – $\text{O}_{\text{ax}}$  distance of 2.35 Å and the four  $\text{Cu}^{2+}$ – $\text{O}_{\text{eq}}$  distances ranging from 2.05 to 2.06 Å. Figure 12 shows the time evolution of the different bond lengths in the  $[\text{CuCl}(\text{H}_2\text{O})_5]^+$  clusters during the 75–125 ps simulation time. The Cu–Cl distance was the longest followed by the Cu– $\text{O}_{\text{ax}}$  distance. The four  $\text{Cu}^{2+}$ – $\text{O}_{\text{eq}}$  distances were shorter on the average with occasional elongations. This elongation of the Cu– $\text{O}_{\text{ax}}$  distance is in agreement with the EXAFS observations reported by D’Angelo et al. in copper chloride solution.<sup>29</sup> We note that a Jahn–Teller distortion<sup>3,14–16</sup> was observed in the  $[\text{Cu}(\text{H}_2\text{O})_6]^{2+}$  clusters in a previous ReaxFF simulation (work in progress). However, the distortion in the current  $[\text{CuCl}(\text{H}_2\text{O})_5]^+$  system cannot be directly attributed to the Jahn–Teller distortion. The presence of mixed ligands ( $\text{Cl}^-$  and  $\text{H}_2\text{O}$ ) already breaks the symmetry of the system. Thus, a Jahn–Teller distortion that attempts to lower the system energy by breaking the symmetry is probably not relevant here. However, it is surprising that a classical force field like ReaxFF can reproduce such distortion that can, in general, only be described by QM. The water coordination of  $\text{CuCl}^+$  derived from this work is in good agreement with the EXAFS data (Table 1 of ref 29) as well as the QM optimized gas phase  $[\text{CuCl}(\text{H}_2\text{O})_5]^+$  cluster (Table 3). However, our

**TABLE 3: Structural Properties of CuCl<sup>+</sup> Solution Derived in This Work As Compared to Reference 29 and the QM Optimized Gas Phase [CuCl(H<sub>2</sub>O)<sub>5</sub>]<sup>+</sup> Cluster in Figure 1**

distances (Å)	CuCl <sup>+</sup> solution simulated by ReaxFF (this work)	EXAFS data (ref 29)	QM optimized gas phase [CuCl(H <sub>2</sub> O) <sub>5</sub> ] <sup>+</sup> cluster (this work)
Cu <sup>2+</sup> –Cl <sup>-</sup>	2.42	2.86	2.40
Cu <sup>2+</sup> –O <sub>axial</sub>	2.25	2.28	2.35
Cu <sup>2+</sup> –O <sub>equatorial</sub>	2.0	1.97	2.06

Cu<sup>2+</sup>–Cl<sup>-</sup> distance of 2.42 Å was shorter than the EXAFS determination of 2.86 Å. Our results are in agreement with the range of values 2.25–2.56 Å found in earlier studies (Table 2 of ref 23).

The average charges on the Cu<sup>2+</sup> and Cl<sup>-</sup> found in the simulation were 1.28 and −0.70, respectively. This shows that the charges from the dication and the anion significantly dissipated to the nearby water molecules, again allowing charge transfer and polarization that are essential to these calculations.

## Conclusion

To facilitate realistic large scale simulations of aqueous chloride and copper chloride, we have developed a ReaxFF reactive force field for Cu–Cl and for Cl–water interactions. To achieve this, we have augmented the training set of a previously developed Cu/O/H potential with the QM optimized geometries of several copper chloride, copper/water/hydroxide, copper/water/chloride, copper/hydroxide, and copper/chloride/water/hydroxide clusters. We have further extended this training set with chloride/water, copper/chloride/water, and copper/chloride/hydroxide/water clusters generated by ReaxFF molecular dynamics simulations. The ReaxFF force field parameters were optimized against this training set. ReaxFF could accurately reproduce the geometries and energies of the complexes.

The structural properties derived by the molecular dynamics simulation of chloride/water system are in excellent agreement with the previous experimental and theoretical results. In particular ReaxFF simulation predicted a chloride ion coordination number of 5 which is close to the preferred experimental value of 6.<sup>69,70,72</sup> Among computational methods, most nonpolarizable classical force fields (Table 2 of ref 69) predict a higher coordination number. A lower coordination number had been achieved by polarizable force fields like Amoeba<sup>74</sup> or computationally expensive methods like QM/MM<sup>69</sup> and CPMD.<sup>73</sup>

The structure of aqueous copper chloride derived by ReaxFF was in excellent accord with the experimental studies performed by D'Angelo et al.<sup>29</sup> This confirmed the reliability of the current force field as a computationally affordable tool that accurately describes aqueous copper chloride including subtle effects like Jahn–Teller distortion. More complex cases, like the effect of multiple chloride ions in the first hydration shell of Cu<sup>2+</sup>, coexistence of multiple oxidation states of copper, and the effect of pH on Cu<sup>2+</sup>–Cl<sup>-</sup> interactions will be the subjects of our future work.

This work establishes the value of ReaxFF as a reactive potential that can accurately simulate ion solvation for dications where polarization and charge transfer effects are essential. Following the schemes developed in this work, ReaxFF model potentials for other metal cations and anions can be developed. These potentials can be utilized to construct a computationally inexpensive tool for large-scale simulations of metal complexes, ore-formation, and metal ion transport with the flexibility to model settings from hydrothermal solutions to biological environments.

**Acknowledgment.** We thank DOE-ORNL-6400007192 for partial support for this work. We also thank Dr. Sandeep Patel for helpful discussions and the reviewers for their valuable comments on this manuscript.

## Appendix

See refs 30 and 54 for the descriptions of the ReaxFF parameters. The following tables provide the ReaxFF parameters optimized in this work.

**TABLE A1: Bond Energy and Bond Order Parameters**

bond	D <sub>e</sub> (kcal/mol)	P <sub>be,1</sub>	P <sub>be,2</sub>	P <sub>ovun1</sub>	P <sub>bo,1</sub>	P <sub>bo,2</sub>
H–Cl	109.17	−0.1657	2.8463	1.25	−0.1111	5.2687
Cu–Cl	118.31	−0.1168	2.9176	0.0697	−0.1316	5.3624

**TABLE A2: van der Waals Interaction and σ-Bond Parameters**

atom pair	ε (kcal/mol)	R <sub>vdW</sub> (Å)	γ <sub>vdW</sub>	R <sub>sigma</sub> (Å)
H–Cl	0.0568	3.348	9.6297	1.2200
O–Cl	0.1927	4.5102	11.2308	<i>a</i>
Cu–Cl	0.1402	4.3208	10.9786	1.7505
Cl–Cl	0.2000	3.8278	11.5345	1.7140

<sup>a</sup> The Cl–O covalent bond was not parametrized in this force field.

**TABLE A3: Charge and atom parameters**

atom type	η (eV)	χ (eV)	γ	p <sub>ov/un</sub>	p <sub>val,3</sub>
Cl	9.9614	6.5316	0.3837	−10.208	2.9867

**TABLE A4: Valence angle parameters**

angle	Θ <sub>o,o</sub> (deg)	p <sub>val,1</sub> (kcal/mol)	p <sub>val,2</sub> (1/radian <sup>2</sup> )	p <sub>val,4</sub>	p <sub>val,7</sub>
O–Cu–Cl	83.31	9.4823	5.7883	2.2640	0.2248
O–Cu–Cl	180.0	3.8549	3.7230	1.04	0.1482
Cu–Cl–Cu	180.0	11.2336	6.8851	1.0893	1.0000
Cu–Cu–Cl	90.0	5.0811	5.2147	1.8538	1.0000
Cl–Cu–Cl	180.0	21.1482	0.3506	1.4361	1.0000
O–H–Cl	180.0	0.01	0.5211	1.3859	0.0000

**TABLE A5: Torsion parameters**

torsion angle	V <sub>1</sub> (kcal/mol)	V <sub>2</sub> (kcal/mol)	V <sub>3</sub> (kcal/mol)	p <sub>tor1</sub>
H–O–Cu–Cl	0.1589	12.50	0.4388	−1.50

## References and Notes

- Pavelka, M.; Simanek, M.; Sponer, J.; Burda, J. V. *J. Phys. Chem. A* **2006**, *110*, 4795.
- Pavelka, M.; Shukla, M. K.; Leszczynski, J.; Burda, J. V. *J. Phys. Chem. A* **2008**, *112*, 256.
- Bersuker, I. B. *The Jahn-Teller effect*; Cambridge University Press: Cambridge, U.K., and New York, 2006.
- Nomura, M.; Yamaguchi, T. *J. Phys. Chem.* **1988**, *92*, 6157.
- Beagley, B.; Eriksson, A.; Lindgren, J.; Persson, I.; Pettersson, L. G. M.; Sandstrom, M.; Wahlgren, U.; White, E. W. *J. Phys.: Condens. Matter* **1989**, *1*, 2395.
- Garcia, J.; Benfatto, M.; Natoli, C. R.; Bianconi, A.; Fontaine, A.; Tolentino, H. *Chem. Phys.* **1989**, *132*, 295.
- Powell, D. H.; Helm, L.; Merbach, A. E. *J. Chem. Phys.* **1991**, *95*, 9258.
- Persson, I.; Persson, P.; Sandstrom, M.; Ullstrom, A. S. *J. Chem. Soc., Dalton Trans.* **2002**, 1256.
- Chaboy, J.; Munoz-Paez, A.; Marcos, E. S. *S. J. Synchrotron Radiat.* **2006**, *13*, 471.
- Chaboy, J.; Munoz-Paez, A.; Merkling, P. J.; Marcos, E. S. *J. Chem. Phys.* **2006**, *124*.
- Benfatto, M.; D'Angelo, P.; Della Longa, S.; Pavel, N. V. *Phys. Rev. B* **2002**, *65*.
- Frank, P.; Benfatto, M.; Szilagyi, R. K.; D'Angelo, P.; Della Longa, S.; Hodgson, K. O. *Inorg. Chem.* **2005**, *44*, 1922.

- (13) Pasquarello, A.; Petri, I.; Salmon, P. S.; Parisel, O.; Car, R.; Toth, E.; Powell, D. H.; Fischer, H. E.; Helm, L.; Merbach, A. E. *Science* **2001**, 291, 856.
- (14) Schwenk, C. F.; Rode, B. M. *ChemPhysChem* **2003**, 4, 931.
- (15) Schwenk, C. F.; Rode, B. M. *Chem. Commun.* **2003**, 1286.
- (16) Schwenk, C. F.; Rode, B. M. *J. Chem. Phys.* **2003**, 119, 9523.
- (17) Burda, J. V.; Pavelka, M.; Simanek, M. *J. Mol. Struct.: THEOCHEM* **2004**, 683, 183.
- (18) Amira, S.; Spangberg, D.; Hermansson, K. *Phys. Chem. Chem. Phys.* **2005**, 7, 2874.
- (19) Pavelka, M.; Burda, J. V. *Chem. Phys.* **2005**, 312, 193.
- (20) Blumberger, J. *J. Am. Chem. Soc.* **2008**, 130, 16065.
- (21) Bryantsev, V. S.; Diallo, M. S.; van Duin, A. C. T.; Goddard, W. A. *J. Phys. Chem. A* **2008**, 112, 9104.
- (22) Smith, D. W. *Coord. Chem. Rev.* **1976**, 21, 93.
- (23) Collings, M. D.; Sherman, D. M.; Ragnarsdottir, K. V. *Chem. Geol.* **2000**, 167, 65.
- (24) Fulton, J. L.; Hoffmann, M. M.; Darab, J. G. *Chem. Phys. Lett.* **2000**, 330, 300.
- (25) Brugger, J.; McPhail, D. C.; Black, J.; Spiccia, L. *Geochim. Cosmochim. Acta* **2001**, 65, 2691.
- (26) Archibald, S. M.; Migdisov, A. A.; Williams-Jones, A. E. *Geochim. Cosmochim. Acta* **2002**, 66, 1611.
- (27) Berry, A. J.; Hack, A. C.; Mavrogenes, J. A.; Newville, M.; Sutton, S. R. *Am. Mineral.* **2006**, 91, 1773.
- (28) Lundstrom, M.; Aromaa, J.; Forsen, O.; Haavanlammi, L. *Acta Metall. Slovaca* **2007**, 3, 447.
- (29) DAngelo, P.; Bottari, E.; Festa, M. R.; Nolting, H. F.; Pavel, N. V. *J. Chem. Phys.* **1997**, 107, 2807.
- (30) van Duin, A. C. T.; Dasgupta, S.; Lorant, F.; Goddard, W. A. *J. Phys. Chem. A* **2001**, 105, 9396.
- (31) Strachan, A.; van Duin, A. C. T.; Chakraborty, D.; Dasgupta, S.; Goddard, W. A. *Phys. Rev. Lett.* **2003**, 91.
- (32) van Duin, A. C. T.; Damste, J. S. S. *Org. Geochem.* **2003**, 34, 515.
- (33) Zhang, Q.; Cagin, T.; van Duin, A.; Goddard, W. A.; Qi, Y.; Hector, L. G. *Phys. Rev. B* **2004**, 69.
- (34) Chenoweth, K.; Cheung, S.; van Duin, A. C. T.; Goddard, W. A.; Kober, E. M. *J. Am. Chem. Soc.* **2005**, 127, 7192.
- (35) Cheung, S.; Deng, W. Q.; van Duin, A. C. T.; Goddard, W. A. *J. Phys. Chem. A* **2005**, 109, 851.
- (36) Han, S. S.; van Duin, A. C. T.; Goddard, W. A.; Lee, H. M. *J. Phys. Chem. A* **2005**, 109, 4575.
- (37) Nielsen, K. D.; van Duin, A. C. T.; Oxgaard, J.; Deng, W. Q.; Goddard, W. A. *J. Phys. Chem. A* **2005**, 109, 493.
- (38) Strachan, A.; Kober, E. M.; van Duin, A. C. T.; Oxgaard, J.; Goddard, W. A. *J. Chem. Phys.* **2005**, 122.
- (39) van Duin, A. C. T.; Zeiri, Y.; Dubnikova, F.; Kosloff, R.; Goddard, W. A. *J. Am. Chem. Soc.* **2005**, 127, 11053.
- (40) Buehler, M. J.; van Duin, A. C. T.; Goddard, W. A. *Phys. Rev. Lett.* **2006**, 96.
- (41) Goddard, W. A.; van Duin, A.; Chenoweth, K.; Cheng, M. J.; Pudar, S.; Oxgaard, J.; Merinov, B.; Jang, Y. H.; Persson, P. *Top. Catal.* **2006**, 38, 93.
- (42) Ludwig, J.; Vlachos, D. G.; van Duin, A. C. T.; Goddard, W. A. *J. Phys. Chem. B* **2006**, 110, 4274.
- (43) Vashishta, P.; Kalia, R. K.; Nakano, A. *J. Phys. Chem. B* **2006**, 110, 3727.
- (44) Chenoweth, K.; van Duin, A. C. T.; Goddard, W. A. *J. Phys. Chem. A* **2008**, 112, 1040.
- (45) Chenoweth, K.; van Duin, A. C. T.; Persson, P.; Cheng, M. J.; Oxgaard, J.; Goddard, W. A. *J. Phys. Chem. C* **2008**, 112, 14645.
- (46) Goddard, W. A.; Chenoweth, K.; Pudar, S.; van Duin, A. C. T.; Cheng, M. J. *Top. Catal.* **2008**, 50, 2.
- (47) Ojwang, J. G. O.; Van Santen, R.; Kramer, G. J.; van Duin, A. C. T.; Goddard, W. A. *J. Chem. Phys.* **2008**, 128.
- (48) Ojwang', J. G. O.; van Santen, R.; Kramer, G. J.; van Duin, A. C. T.; Goddard, W. A. *J. Chem. Phys.* **2008**, 129.
- (49) Raymand, D.; van Duin, A. C. T.; Baudin, M.; Hermansson, K. *Surf. Sci.* **2008**, 602, 1020.
- (50) van Duin, A. C. T.; Merinov, B. V.; Han, S. S.; Dorso, C. O.; Goddard, W. A. *J. Phys. Chem. A* **2008**, 112, 11414.
- (51) van Duin, A. C. T.; Merinov, B. V.; Jang, S. S.; Goddard, W. A. *J. Phys. Chem. A* **2008**, 112, 3133.
- (52) Zhu, R.; Janetko, F.; Zhang, Y.; van Duin, A. C. T.; Goddard, W. A.; Salahub, D. R. *Theor. Chem. Acc.* **2008**, 120, 479.
- (53) Mortier, W. J.; Ghosh, S. K.; Shankar, S. *J. Am. Chem. Soc.* **1986**, 108, 4315.
- (54) van Duin, A. C. T.; Strachan, A.; Stewman, S.; Zhang, Q. S.; Xu, X.; Goddard, W. A. *J. Phys. Chem. A* **2003**, 107, 3803.
- (55) Lee, C. T.; Yang, W. T.; Parr, R. G. *Phys. Rev. B* **1988**, 37, 785.
- (56) Becke, A. D. *J. Chem. Phys.* **1993**, 98, 5648.
- (57) Perdew, J. P.; Burke, K.; Ernzerhof, M. *Phys. Rev. Lett.* **1996**, 77, 3865.
- (58) Schultz, P. A. SeqQuest, Sandia National Labs, Alburquerque, NM, <http://dft.sandia.gov/Quest/>.
- (59) Wood, R. H.; Yezdimer, E. M.; Sakane, S.; Barriocanal, J. A.; Doren, D. *J. J. Chem. Phys.* **1999**, 110, 1329.
- (60) Goddard, P. J.; Lambert, R. M. *Surf. Sci.* **1977**, 67, 180.
- (61) Walter, W. K.; Manolopoulos, D. E.; Jones, R. G. *Surf. Sci.* **1996**, 348, 115.
- (62) Broekmann, P.; Wilms, M.; Kruft, M.; Stuhlmann, C.; Wandelt, K. *J. Electroanal. Chem.* **1999**, 467, 307.
- (63) Doll, K.; Harrison, N. M. *Chem. Phys. Lett.* **2000**, 317, 282.
- (64) Re, S.; Osamura, Y.; Suzuki, Y.; Schaefer, H. F. *J. Chem. Phys.* **1998**, 109, 973.
- (65) Milet, A.; Struniewicz, C.; Moszynski, R.; Wormer, P. E. S. *J. Chem. Phys.* **2001**, 115, 349.
- (66) Cabaleiro-Lago, E. M.; Hermida-Ramon, J. M.; Rodriguez-Otero, J. *J. Chem. Phys.* **2002**, 117, 3160.
- (67) Odde, S.; Mhin, B. J.; Lee, S.; Lee, H. M.; Kim, K. S. *J. Chem. Phys.* **2004**, 120, 9524.
- (68) Gutberlet, A.; Schwaab, G.; Birer, O.; Masia, M.; Kaczmarek, A.; Forbert, H.; Havenith, M.; Marx, D. *Science* **2009**, 324, 1545.
- (69) Tongraar, A.; Rode, B. M. *Phys. Chem. Chem. Phys.* **2003**, 5, 357.
- (70) Ohtaki, H.; Radnai, T. *Chem. Rev.* **1993**, 93, 1157.
- (71) Kameda, Y.; Usuki, T.; Uemura, O. *Bull. Chem. Soc. Jpn.* **1998**, 71, 1305.
- (72) Neilson, G. W.; Tromp, R. H. *Annu. Rep. Prog. Chem., Sect. C: Phys. Chem.* **1991**, 88, 45.
- (73) Heuft, J. M.; Meijer, E. J. *J. J. Chem. Phys.* **2003**, 119, 11788.
- (74) Laage, D.; Hynes, J. T. *Proc. Natl. Acad. Sci. U.S.A.* **2007**, 104, 11167.
- (75) Kropman, M. F.; Bakker, H. J. *Science* **2001**, 291, 2118.
- (76) Kropman, M. F.; Bakker, H. J. *J. J. Chem. Phys.* **2001**, 115, 8942.
- (77) Tongraar, A.; Rode, B. M. *Chem. Phys. Lett.* **2005**, 403, 314.
- (78) Ramette, R. W.; Fan, G. *Inorg. Chem.* **1983**, 22, 3323.
- (79) Humphrey, W.; Dalke, A.; Schulten, K. *J. Mol. Graphics* **1996**, 14, 33.

JP9090415